

Performance analysis of field oriented controlled PMSM based electric truck

Sanskriti Achary, Rutul Chaudhari, Siddharthsingh K. Chauhan

Department of Electrical Engineering, Institute of Technology, Nirma University, Ahmedabad, India

Article Info

Article history:

Received Mar 25, 2024

Revised Jun 22, 2024

Accepted Aug 8, 2024

Keywords:

Charging

Electric truck

PMSM

Powertrain

Regenerative braking

ABSTRACT

The electric vehicle (EV) concept is considered the ideal solution to save the environment from pollution occurring due to internal combustion engines or ICE-based vehicles. However, electric power trains have found more penetration in the segment of passenger vehicles and electric buses. This paper presents the performance of an electric truck. Field-oriented controlled permanent magnet synchronous motor (PMSM) is used for the powertrain of the proposed electric truck. The performance of the proposed electric truck is analyzed for propulsion as well as regenerative mode of operation using MATLAB. The effect of different gradient conditions of the road surface on the behavior of the proposed truck is observed. The presented simulation results depict the satisfactory operation of the proposed PMSM-driven electric truck for various operating conditions.

This is an open access article under the [CC BY-SA](#) license.



Corresponding Author:

Siddharthsingh K. Chauhan

Department of Electrical Engineering, Institute of Technology, Nirma University

Ahmedabad, Gujarat, India

Email: siddharthsingh.chauhan@nirmauni.ac.in

1. INTRODUCTION

The massive effect of pollution due to conventional vehicles (i.e., internal combustion engine-based vehicles) is very well known and has now become one of the dominant causes of global warming. Along with the environmental benefits offered by an electric vehicle, qualities like smooth driving, noiseless driving, more enjoyable driving experience, and much more can be achieved [1]. This becomes the reason battery-powered electric vehicles are being promoted globally by various countries.

As commercial vehicles are a considerable proportion of the vehicular segment, along with electrical vehicle (EV) cars, the trend of electric buses and trucks is also now increasing. Also, certain case studies like in [2] regarding cross docking EV trucks prove the enhancement of energy efficiency by 40% along with limiting greenhouse gases (GHG) emissions by 30%. Like an EV car, for an electric truck, it becomes important to choose the feasible powertrain and drivetrain configuration to achieve better control of the vehicle [3]-[5].

In this paper, one such powertrain with regenerative braking is simulated. The suitable vehicle parameters have been chosen for each component of the powertrain. The modeling uses the field-oriented control (FOC) control strategy for the permanent magnet synchronous motor (PMSM)-based electric truck. The experiment with different gradients has been analyzed in this paper to observe the efficiency of the proposed powertrain for a standard FTP72 drive cycle in MATLAB Simulink R2023a environment. The presented results will help the researchers to analyze the behavior of electric trucks under various operating conditions.

2. POWERTRAIN ARCHITECTURE AND DRIVETRAIN OF ELECTRIC TRUCK

The powertrain is a configuration that involves power electronic converters, motors, and a further transmission system to the wheels of the vehicle. Powertrain architecture can be expressed in different manners, one such form is expressed in below block diagram of Figure 1. As shown in the figure, the electronics controller (EC) collects the user input and sensor data from the battery and processes it appropriately to supply it to other components of the powertrain. The energy management unit (EMU) ensures safe operation by preventing overcharging, over-discharging, and thermal runaway by monitoring various battery parameters. An energy refueling unit (ERU) refers to either an onboard charger or an offboard charger through which the transfer of energy to the EV from the grid can be achieved. The auxiliary supply and the temperature control unit are required for power steering and EV environment control respectively. Depending upon the type of motor, an appropriate power electronic converter fed from the battery is used to supply the said motor with variable voltage and frequency supply, which in turn helps to control the motor's speed and torque. The configuration ahead of the motor depends upon the drivetrain configuration possibilities [6]-[9]. Though having some similarities in powertrains of EV trucks and cars similar to Figure 1, they have some key differences: i) Trucks demand larger battery packs and more powerful motors than cars to tackle heavier loads and challenging terrain; ii) Trucks leverage multi-speed transmissions rather than single-speed as in cars, which enhances control across various conditions like powerful low-speed pulling; and iii) EV trucks often require more robust cooling systems for the motor, battery pack, and power electronics compared to cars. Along with the powertrain, gross vehicle weight rating (GVWR) is another factor in differentiating the design of the trucks. Table 1 presents the classification of vehicles based on the GVWR.

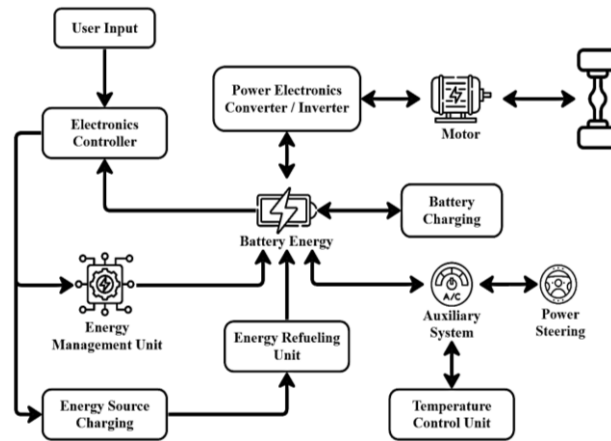


Figure 1. Powertrain block diagram of electric truck

Table 1. Classification of vehicles based on GVWR

| Class | GVWR (lbs) | Type/application of vehicle |
|--------------|-------------|---|
| Class-1 to 3 | <14000 | Car, sport utility vehicle or SUV, and non-commercial pick-up truck |
| Class-4 | 14000-16000 | Box truck and delivery truck |
| Class-5 | 16000-19500 | Bucket truck |
| Class-6 | 19500-26000 | Beverage truck and school bus |
| Class-7 | 26000-33000 | Sweeper truck |
| Class-8 | >33000 | Cement truck and long trailer truck |

2.1. Different drivetrain configurations

The drivetrain is the subset of a powertrain. Among different configurations like front-wheel drive (FWD), rear-wheel drive (RWD), four-wheel drive (4WD), and all-wheel drive (AWD), for trucks, RWD is preferred as it provides a better distribution of weight and better acceleration. In this paper, we have considered the powertrain with a single motor for simulation [10].

2.2. Comparison of different motors

The motor should have high torque with low ripple and wide-speed range, good maximum speed-to-base speed ratio, high efficiency, high reliability, and robustness [11]-[15]. Among various EV motors like permanent magnet synchronous motor (PMSM), switched reluctance motor (SRM), direct current motor

(DCM), and induction motor (IM), PMSM is preferred for EV trucks. Table 2 shows the comparison of different EV motors ('↑' shows that the motor is more compatible whereas '↓' shows less compatibility regarding the mentioned parameters) [8].

Table 2. Comparison of EV motors

| Parameters | DCM | IM | Brushless DC electric motor (BLDC) | PMSM |
|-------------------------------|-----|----|------------------------------------|------|
| Torque/power density | ↓ | - | ↑↑ | ↑↑ |
| Efficiency | ↓ | ↑↑ | ↑↑ | ↑↑ |
| Cost beneficial | - | ↑↑ | ↓ | ↓ |
| Reliability | ↓ | ↑↑ | ↑↑ | ↑↑ |
| Size/weight/volume | ↓ | ↑ | ↑↑ | ↑↑ |
| Overload capability | ↓ | ↑ | ↑ | ↑ |
| Field weakening | ↑↑ | ↑↑ | ↓ | ↑ |
| Fault tolerance | ↑↑ | ↑↑ | ↓ | ↓ |
| Thermal limitation | ↓ | ↑ | ↓ | ↓ |
| Noise/vibration/torque ripple | ↓ | ↑↑ | - | ↑↑ |
| Lifetime | ↓ | ↑↑ | ↑ | ↑ |
| Future potential | ↓ | ↑↑ | - | ↑↑ |

3. METHOD

MATLAB Simulink R2023a is used as a simulation environment. Figure 2 shows the powertrain schematic of an EV truck that can perform regenerative braking. The developed simulation model is shown in Figure 3. The powertrain works according to the comparison between the drive cycle and the feedback received from the vehicle velocity; the driver will accelerate or decelerate the vehicle with the help of the control and electronics involved [16], [17]. Energy from the battery is fed to the PMSM motor which is further connected to the mechanical assembly of the vehicle. Here, the FTP72 drive cycle is used as the reference speed. A longitudinal driver block is used which generates acceleration and deceleration commands according to the error between reference speed and the feedback obtained from the vehicle. Further, the signal is compared with the motor's speed which is then fed to the FOC control loop where the torque component of current from the FOC subsystem is compared [18]. Parameters for the simulation are considered as per Table 3.

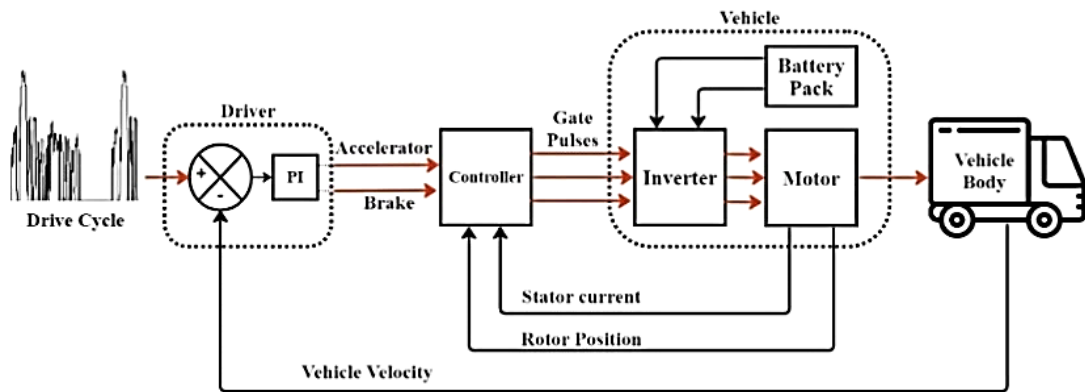


Figure 2. Schematic of EV truck

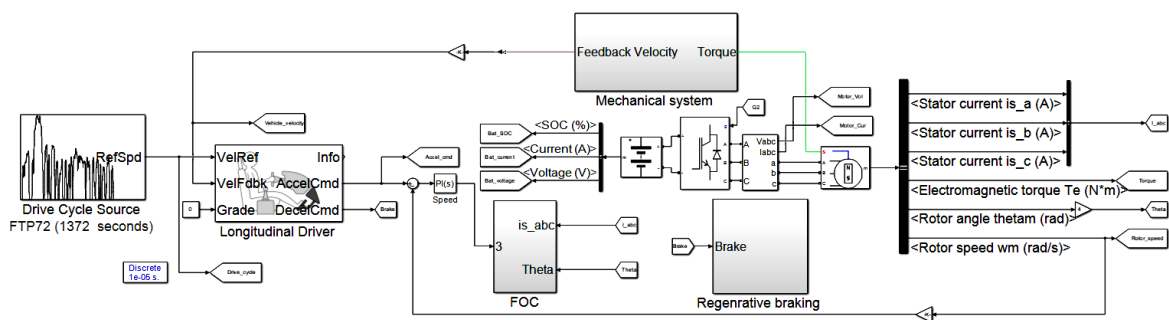


Figure 3. Simulation model of EV truck powertrain

3.1. Controller strategy

FOC offers a sophisticated method for controlling alternating current (AC) motors, mimicking the behavior of direct current (DC) motors. It achieves decoupled torque and speed control through Clarke transformation ($a, b, c \rightarrow \alpha, \beta$) as in (1)-(3) and Park transformation ($\alpha, \beta \rightarrow d, q$) as in (4)-(5). This can be observed in Figure 4. After getting FOC, pulses are generated using the space vector pulse width modulation (SVPWM) method [19], [20]. The primary principle of SVPWM focuses on creating an average voltage vector within the switching cycle that will be compatible with the required output voltage for the motor. SVPWM is preferred over sinusoidal pulse width modulation (SPWM) for FOC due to its efficient performance and controllability [21], [22].

$$i_\alpha = \frac{2}{3} i_a - \frac{1}{3} (i_b + i_c) \quad (1)$$

$$i_\beta = \frac{2}{\sqrt{3}} (i_b - i_c) \quad (2)$$

$$i_0 = \frac{2}{3} (i_a + i_b + i_c) \quad (3)$$

$$i_{sd} = i_\alpha \cos(\theta) + i_\beta \sin(\theta) \quad (4)$$

$$i_{sq} = -i_\alpha \sin(\theta) + i_\beta \cos(\theta) \quad (5)$$

Table 3. System parameters considered for simulation

| Parameters | Values | Parameters | Values |
|--------------------------------|---------------------|------------------------------------|-------------------------|
| Vehicle mass | 3055 kg | Motor armature inductance | 420 μ H |
| Aerodynamic drag coefficient | 0.4 | Motor inertia | 0.864 kg.m ² |
| Rolling resistance coefficient | 0.022 | Torque constant | 1.842 N.m/A |
| Vehicle frontal area | 3.82 m ² | Internal resistance of the battery | 0.04 Ω |
| Radius of wheel | 0.405 m | Battery capacity | 100 Ah |
| Gear ratio | 3 | Battery nominal voltage | 400 V |
| Motor stator phase resistance | 0.0045 Ω | | |

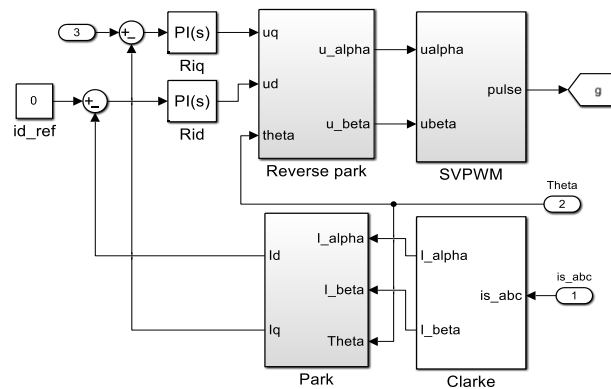


Figure 4. FOC of EV truck

3.2. Mechanical body of EV truck

The vehicle's mechanical body as shown in Figure 5 consists of a torque sensor, gear assembly, brake, and four tires. The torque sensor translates a variable into a proportional torque control signal. The gearbox maintains a fixed gear ratio, while the brake uses an actuator to control deceleration based on driver input. Finally, the four tires consider inertia, rolling resistance, and compliance to represent real-world tire behavior. Velocity from the vehicle body block is given as feedback to the driver which then gets compared with the drive-cycle [23].

3.3. Regenerative braking

Regenerative braking is the crucial goal to be achieved by any EV. Here whenever the driver gives the deceleration command, regenerative braking occurs and the state of charge (SOC) of the battery gets increased [24]-[27]. The percentage of increment in SOC would depend upon the slope of the deceleration

4. RESULT AND DISCUSSION

In this paper, three different cases are considered for analyzing the performance of EV trucks. The three cases are based on different gradients thereby demonstrating the way the proposed EV truck responds to follow the reference drive cycle.

4.1. Case i: EV truck performance with a gradient of 0°

This case depicts that the truck is moving on a path with zero gradient and is assumed that the vehicle follows the drive cycle with necessary acceleration and deceleration commands. As can be seen in Figure 7(a), drive cycle FTP72 has been used as a reference velocity for 200 seconds and when vehicle velocity is compared, it follows the same as shown in Figure 7(b). Figure 7(c) shows the deceleration command given when there is a deep in the drive cycle. Due to this deceleration command, regenerative braking occurs and leads to an increase in (%) SOC of the battery. This can be observed in Figure 7(d). Figures 8(a)-8(c) show this behavior for 15 seconds of the FTP72 drive cycle.

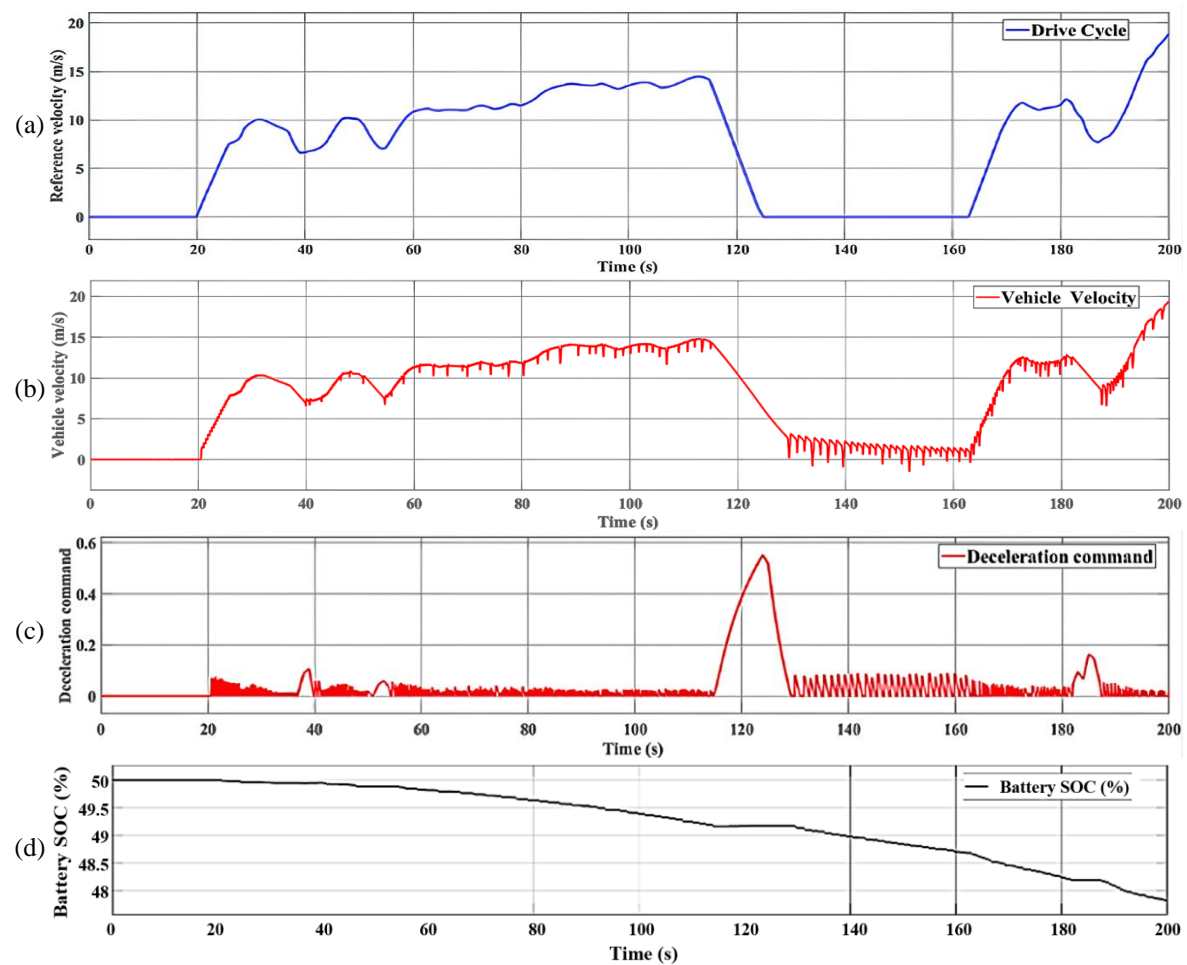


Figure 7. Comparison of drive cycle and vehicle velocity: (a) drive cycle [scale: y-axis-5 (m/s)/div.; x-axis-20 s/div.], (b) vehicle velocity [scale: y-axis-5 (m/s)/div.; x-axis-20s/div.], (c) deceleration command [scale: y-axis-0.2 per div.; x-axis-20 s/div.], and (d) battery SOC (%) [scale: y-axis-0.5 %/div.; x-axis-20 s/div.]

4.2. Case ii: vehicle with a gradient of 20°

This case represents the scenario where a gradient of 20° is given to the vehicle. Due to the gradient of 20° , the driver will not be able to catch the speed as per the reference (drive cycle) shown in Figure 7(a). After some seconds have passed, when the reference velocity boosts to some level then only the driver starts to give acceleration command and will try to get close to reference velocity as much as possible. As there is no

need for a brake pedal in this case, there will not be any increment in the level of SOC of the battery. Figure 9(a) shows the result for torque constant=1.8421, whereas Figure 9(b) shows the acceleration command given by the driver which faces initial lag due to the inherent inertia of the vehicle. If the value of torque constant is increased to 4 then the driver can achieve stable velocity earlier than the previous case which is shown in Figure 10. For safety, the vehicle control is designed so as to restrict the velocity to 30 m/s during uphill operation.

4.3. Case iii: vehicle with a gradient of -20°

The vehicle is moving downhill slope of -20° causing the vehicle to accelerate as shown in Figure 11(a). To maintain the reference velocity, the driver brakes to prevent unwanted acceleration as shown in Figure 11(b). This braking utilizes regenerative braking; hence battery state of charge (SOC) will start increasing as shown in Figure 11(c). In this scenario, additional acceleration is not required, so the acceleration command will be zero. The vehicle control is designed so as to restrict the velocity to 30 m/s during downhill operation.

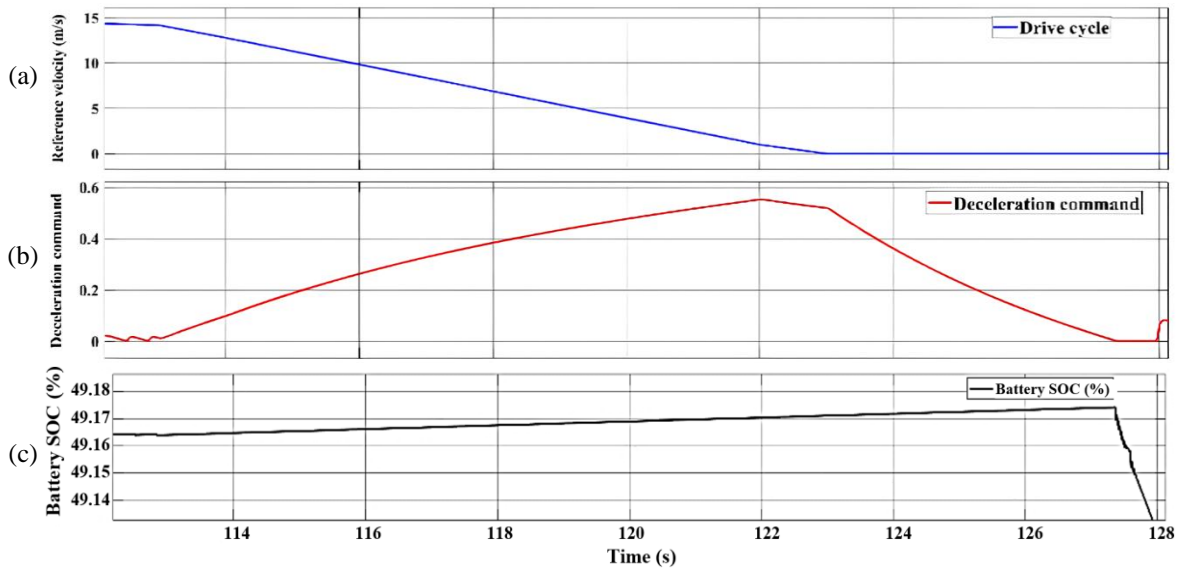


Figure 8. Drive cycle, deceleration command, and battery SOC for 15 seconds: (a) drive cycle [scale: y-axis-5 (m/s)/div.; x-axis-2 s/div.], (b) deceleration command [scale: y-axis-0.2 per div.; x-axis-2 s/div.], and (c) battery SOC (%) [scale: y-axis-0.01%/div.; x-axis-2 s/div.]

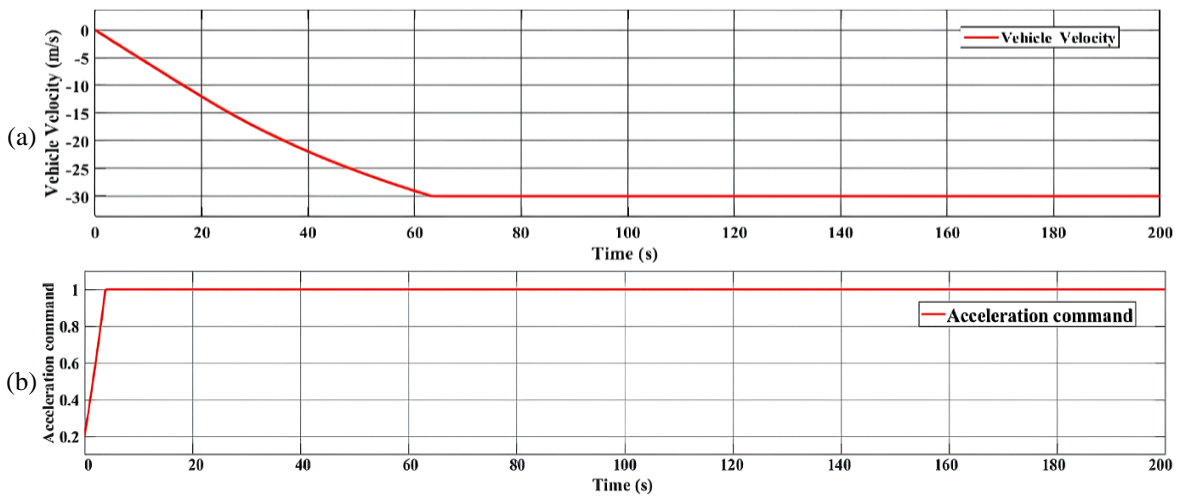


Figure 9. Drive cycle and vehicle velocity for the gradient of 20° (torque constant=1.8421): (a) vehicle velocity [scale: y-axis-5 (m/s)/div.; x-axis-20 s/div.] and (b) acceleration command [scale: y-axis-0.2 per div.; x-axis-20 s/div.]

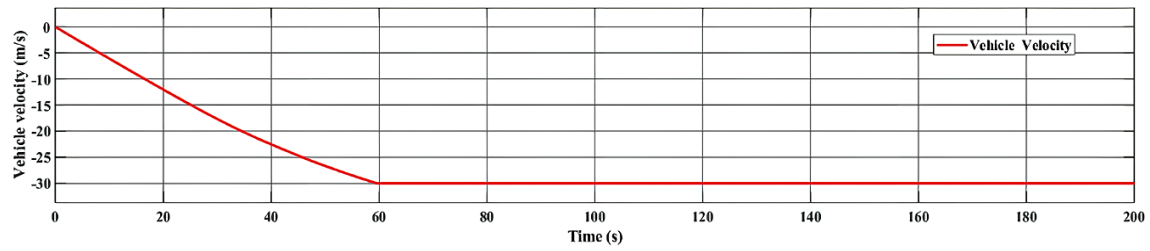


Figure 10. Vehicle velocity for the gradient of 20° (torque constant = 4): [scale: y-axis-5 (m/s)/div.; x-axis-20 s/div.]

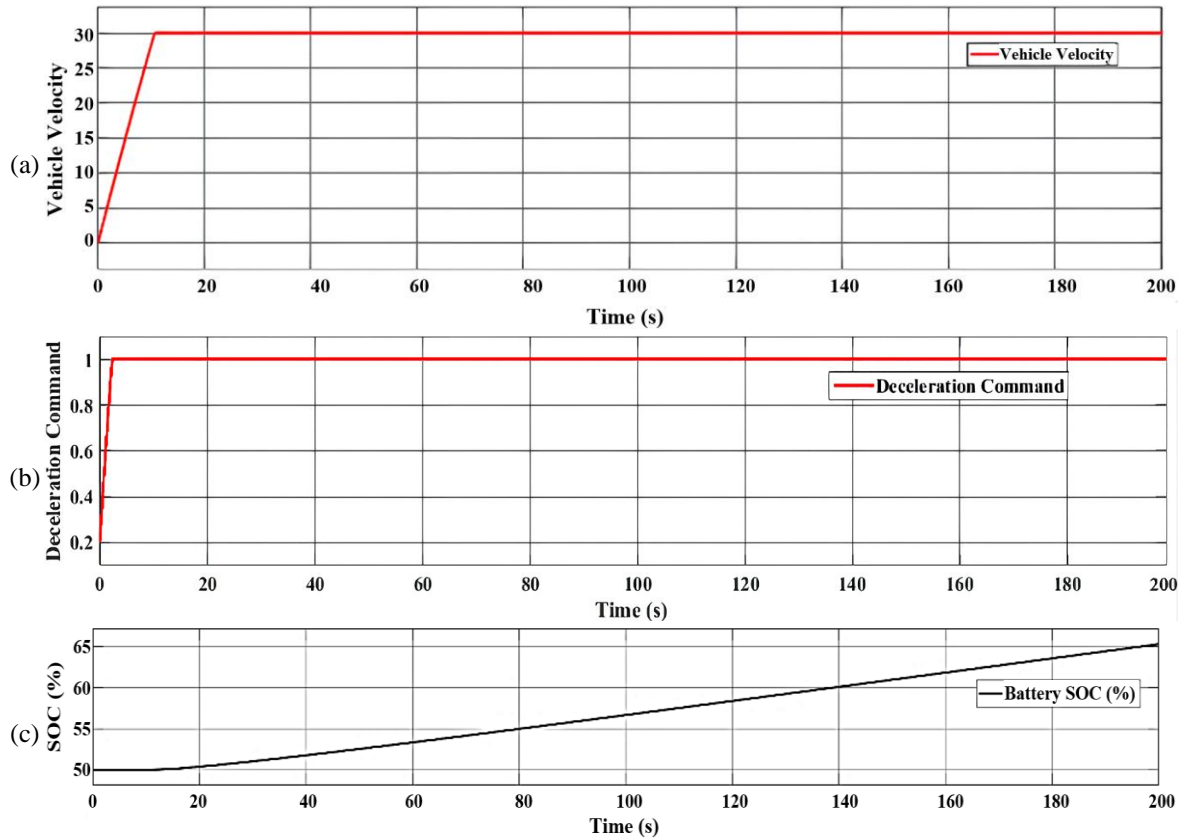


Figure 11. Drive cycle, deceleration command, and battery SOC for the gradient of -20° : (a) vehicle velocity [scale: y-axis-5 (m/s)/div.; x-axis-20 s/div.], (b) deceleration command [scale: y-axis-0.2 per div.; x-axis- 20 s/div.], and (c) battery SOC (%) [scale: y-axis- 5%/div.; x-axis- 20 s/div.]

5. CONCLUSION

Performance analysis of an electric truck propelled by a permanent magnet synchronous motor is presented in this paper. The field-oriented control method is used for controlling the motor of the proposed electric truck. MATLAB-based simulation analysis for evaluation of the performance of the proposed electric truck is carried out. Standard drive cycle FTP72 is used to evaluate the response of the presented electric truck for conditions of acceleration as well as deceleration. Along with the vehicle speed, the SOC of the battery is also observed for different vehicle speed conditions as affected by the considered drive cycle. Results depict the effective operation of the truck both during conditions of propulsion and regenerative braking. Effective augmentation of battery SOC is observed during regenerative braking of the truck. The performance of the proposed electric truck is also analyzed for surfaces with different gradients which helps in reinstating the significance of the appropriate selection of motor torque constant which is directly linked with the acceleration capability of the truck. Similar work can be carried out for the hybrid model of the truck, a truck with a 4WD configuration, also the integration of a piezo circuit can enhance the battery capacity and eventually the range of the truck.




REFERENCES

- [1] L. N. Patil and H. P. Khairnar, "Investigation of perceived risk encountered by electric vehicle drivers in distinct contexts," *Applied Engineering Letters: Journal of Engineering and Applied Sciences*, vol. 6, no. 2, pp. 69–79, 2021, doi: 10.18485/aeletters.2021.6.2.4.
- [2] Á. Bányai, "Energy-efficiency and sustainability in cross-docking supply using e-vehicles," *Applied Engineering Letters: Journal of Engineering and Applied Sciences*, vol. 8, no. 4, pp. 139–147, 2023, doi: 10.18485/aeletters.2023.8.4.1.
- [3] M. Ackerl, M. Kordon, H. Schreier, H. Petutschnig, and M. Huetter, "Route to electrification for trucks & busses in India," in *2017 IEEE Transportation Electrification Conference (ITEC-India)*, IEEE, Dec. 2017, pp. 1–6. doi: 10.1109/ITEC-India.2017.8333856.
- [4] H. Weiss, T. Winkler, and H. Ziegerhofer, "Large lithium-ion battery-powered electric vehicles — From idea to reality," in *2018 ELEKTRO*, IEEE, May 2018, pp. 1–5. doi: 10.1109/ELEKTRO.2018.8398241.
- [5] B. A. Davis and M. A. Figliozzi, "A methodology to evaluate the competitiveness of electric delivery trucks," *Transportation Research Part E: Logistics and Transportation Review*, vol. 49, no. 1, pp. 8–23, Jan. 2013, doi: 10.1016/j.tre.2012.07.003.
- [6] S. Wolff, S. Kalt, M. Bstieler, and M. Lienkamp, "Influence of powertrain topology and electric machine design on efficiency of battery electric trucks—a simulative case-study," *Energies*, vol. 14, no. 2, p. 328, Jan. 2021, doi: 10.3390/en14020328.
- [7] A. Karki, S. Phuyal, D. Tuladhar, S. Basnet, and B. Shrestha, "Status of pure electric vehicle power train technology and future prospects," *Applied System Innovation*, vol. 3, no. 3, p. 35, Aug. 2020, doi: 10.3390/asi3030035.
- [8] S. Madichetty, A. J. Neroth, S. Mishra, and B. C. Babu, "Route towards road freight electrification in india: examining battery electric truck powertrain and energy consumption," *Chinese Journal of Electrical Engineering*, vol. 8, no. 3, pp. 57–75, Sep. 2022, doi: 10.23919/CJEE.2022.000026.
- [9] G. Di Ilio, P. Di Giorgio, L. Tribioli, G. Bella, and E. Jannelli, "Preliminary design of a fuel cell/battery hybrid powertrain for a heavy-duty yard truck for port logistics," *Energy Conversion and Management*, vol. 243, p. 114423, Sep. 2021, doi: 10.1016/j.enconman.2021.114423.
- [10] A. Kampker, R. Pandey, J. G. D. Gomez, S. Wessel, P.-E. Treichel, and I. Malatyali, "Cost optimal design strategy of electric drivetrains for medium heavy-duty vehicles based on product development and production costs," in *2019 9th International Electric Drives Production Conference (EDPC)*, IEEE, Dec. 2019, pp. 1–8. doi: 10.1109/EDPC48408.2019.9011844.
- [11] V. Dmitrievskii, V. Prakht, E. Valeev, A. Paramonov, V. Kazakbaev, and A. Anuchin, "Comparative study of induction and wound rotor synchronous motors for the traction drive of a mining dump truck operating in wide constant power speed range," *IEEE Access*, vol. 11, pp. 68395–68409, 2023, doi: 10.1109/ACCESS.2023.3292244.
- [12] S. Krishnamoorthy and P. P. K. Panikkar, "A comprehensive review of different electric motors for electric vehicles application," *International Journal of Power Electronics and Drive Systems (IJPEDS)*, vol. 15, no. 1, pp. 74–90, Mar. 2024, doi: 10.11591/ijpeds.v15.i1.pp74-90.
- [13] I. Dvornikovs, M. Marinbahs, J. Zarembo, E. Groza, and K. Ketners, "Investigation of traction motor dynamic using computer simulation and method of mutual loading of two pair motors," in *2019 16th Conference on Electrical Machines, Drives and Power Systems (ELMA)*, IEEE, Jun. 2019, pp. 1–4. doi: 10.1109/ELMA.2019.8771518.
- [14] K. Odo, C. Ohanu, I. Chinaeke-Ogbuka, A. Ajibo, C. Ogbuka, and E. Ejiogu, "A novel direct torque and flux control of permanent magnet synchronous motor with analytically-tuned PI controllers," *International Journal of Power Electronics and Drive Systems (IJPEDS)*, vol. 12, no. 4, pp. 2103–2112, Dec. 2021, doi: 10.11591/ijpeds.v12.i4.pp2103-2112.
- [15] R. M. A. V. G. and M. V. P., "Virtual modelling and loss study of permanent magnet synchronous motor used in electric pickup truck," in *2023 International Conference on Control, Communication and Computing (ICCC)*, IEEE, May 2023, pp. 1–6. doi: 10.1109/ICCC57789.2023.10165373.
- [16] S. Singirikonda and O. Yeddula Pedda, "Investigation on performance evaluation of electric vehicle batteries under different drive cycles," *Journal of Energy Storage*, vol. 63, p. 106966, Jul. 2023, doi: 10.1016/j.est.2023.106966.
- [17] D. Maamria, K. Gillet, G. Colin, Y. Chamailard, and C. Nouillant, "Optimal predictive eco-driving cycles for conventional, electric, and hybrid electric cars," *IEEE Transactions on Vehicular Technology*, vol. 68, no. 7, pp. 6320–6330, Jul. 2019, doi: 10.1109/TVT.2019.2914256.
- [18] L. Yu, C. Wang, H. Shi, R. Xin, and L. Wang, "Simulation of PMSM field-oriented control based on SVPWM," in *2017 29th Chinese Control And Decision Conference (CCDC)*, IEEE, May 2017, pp. 7407–7411. doi: 10.1109/CCDC.2017.7978524.
- [19] W.-T. Franke, B. Carstens, F. W. Fuchs, and N. Eggert, "A detailed analysis of a power converter to buffer the battery voltage in lift trucks," in *2009 35th Annual Conference of IEEE Industrial Electronics*, IEEE, Nov. 2009, pp. 31–36. doi: 10.1109/IECON.2009.5414801.
- [20] J. YingYing, W. XuDong, M. LiangLiang, Y. ShuCai, and Z. HaiXing, "Application and simulation of SVPWM in three phase inverter," in *Proceedings of 2011 6th International Forum on Strategic Technology*, IEEE, Aug. 2011, pp. 541–544. doi: 10.1109/IFOST.2011.6021082.
- [21] A. Iqbal, A. Lamine, I. Ashraf, and Mohibullah, "Matlab/Simulink model of space vector PWM for three-phase voltage source inverter," in *Proceedings of the 41st International Universities Power Engineering Conference*, IEEE, Sep. 2006, pp. 1096–1100. doi: 10.1109/UPEC.2006.367646.
- [22] Z. Bin Ibrahim, M. L. Hossain, I. Bin Bugis, N. M. N. Mahadi, and A. Shukri, "Simulation investigation of SPWM, THIPWM and SVPWM techniques for three phase voltage source inverter," *International Journal of Power Electronics and Drive System (IJPEDS)*, vol. 4, no. 2, pp. 223–232, 2014, doi: 10.11591/ijpeds.v4i2.583.
- [23] L. Lindgren, A. Grauers, J. Ranggård, and R. Mäki, "Drive-cycle simulations of battery-electric large haul trucks for open-pit mining with electric roads," *Energies*, vol. 15, no. 13, p. 4871, Jul. 2022, doi: 10.3390/en15134871.
- [24] D. K. Sandilya, S. Goswami, B. Kalita, and S. Chakraborty, "A study on regenerative braking system with Matlab simulation," in *2017 International Conference on Intelligent Computing and Control (I2C2)*, IEEE, Jun. 2017, pp. 1–6. doi: 10.1109/I2C2.2017.8321879.
- [25] R. Razi, K. Hajar, A. Hably, M. Mehrasa, S. Bacha, and A. Labonne, "Assessment of predictive smart charging for electric trucks: a case study in fast private charging stations," in *2022 IEEE International Conference on Electrical Sciences and Technologies in Maghreb (CISTEM)*, IEEE, Oct. 2022, pp. 1–6. doi: 10.1109/CISTEM55808.2022.10043874.
- [26] K. Walz, F. Otteny, and K. Rudion, "A charging profile modeling approach for battery-electric trucks based on trip chain generation," in *2021 IEEE PES Innovative Smart Grid Technologies Europe (ISGT Europe)*, IEEE, Oct. 2021, pp. 1–5. doi: 10.1109/ISGTEurope52324.2021.9640136.
- [27] J. Linru, Z. Yuanxing, L. Taoyong, D. Xiaohong, and Z. Jing, "Analysis on charging safety and optimization of electric vehicles," in *2020 IEEE 6th International Conference on Computer and Communications (ICCC)*, IEEE, Dec. 2020, pp. 2382–2385. doi: 10.1109/ICCC51575.2020.9344906.




- [28] C. S. Boopathi, S. Saha, A. Singh, and S. Sinha, "Regenerative braking in electric vehicles," *International Journal of Recent Technology and Engineering*, vol. 8, no. 2S11, pp. 3338–3346, Nov. 2019, doi: 10.35940/ijrte.B1562.0982S1119.
- [29] V. Totev and V. Gueorgiev, "Modelling of regenerative braking," in *2021 17th Conference on Electrical Machines, Drives and Power Systems (ELMA)*, IEEE, Jul. 2021, pp. 1–6. doi: 10.1109/ELMA52514.2021.9502983.

BIOGRAPHIES OF AUTHORS






Sanskruti Achary    is a final-year engineering student pursuing a B.Tech. in Electrical Engineering from the Institute of Technology, Nirma University, Ahmedabad, Gujarat, India. Her research interests are power electronics, motor drives, electric vehicles, and the automobile sector. She can be contacted at email: 20bee004@nirmauni.ac.in or gj22129@gmail.com.



Rutul Chaudhari    is a final-year engineering student pursuing a B.Tech. in Electrical Engineering from the Institute of Technology, Nirma University, Ahmedabad, Gujarat, India. His research interests include power electronics, electric vehicles, PV systems, and artificial intelligence. He can be contacted at email: 20bee023@nirmauni.ac.in or rutul2122003@gmail.com.



Siddharthsingh K. Chauhan    received his B.E., M.E., & Ph.D. in 2003, 2005, and 2014, respectively, in the field of Electrical Engineering. He is presently working as an associate professor at the Department of Electrical Engineering, Institute of Technology, Nirma University. He is a senior member of IEEE. His research areas include power quality improvement devices, advanced current controllers, digital signal processor-based power electronic systems, power electronics applications to power systems, and applications of artificial intelligence to power electronic systems. He can be contacted at email: siddharthsingh.chauhan@nirmauni.ac.in.